energies

Article

Coordinated Optimization Method for Distributed Energy Storage and Dynamic Reconfiguration to Enhance the Economy and Reliability of Distribution Network

Caihong Zhao [1], Qing Duan [1], Junda Lu [2,*], Haoqing Wang [1], Guanglin Sha [1], Jiaoxin Jia [2,*] and Qi Zhou [3]

1 Country Distribution Technology Center, China Electric Power Research Institute, Beijing 100192, China; zhaocaihong@epri.sgcc.com.cn (C.Z.); duanqing@epri.sgcc.com.cn (Q.D.); wanghaoqing@epri.sgcc.com.cn (H.W.); shaguanglin@epri.sgcc.com.cn (G.S.)
2 Key Laboratory of Distributed Energy Storage and Micro-Grid of Hebei Province, North China Electric Power University, Baoding 071003, China
3 Electric Power Science Research Institute of State Grid Jiangsu Electric Power Company, Nanjing 211103, China; dianqizhouqi@163.com
* Correspondence: 120222101039@ncepu.edu.cn (J.L.); jiajx33@163.com (J.J.)

Abstract: To fully leverage the application potential of distributed energy storage systems (DESS) and network reconfiguration, a coordinated optimization method is proposed to enhance the economic efficiency of distribution networks under normal conditions and the reliability of a power supply during fault conditions. First, a scenario-generation method is developed based on Latin hypercube sampling and Kantorovich distance synchronous back-substitution reduction is used to obtain the typical scenario of wind and solar output. Next, a planning operation coordinated optimization framework and model are established, considering both normal and fault states of the distribution network. In the planning layer, the objective is to minimize the annual comprehensive capital expenditures for the distribution network to improve the economic efficiency of the distribution network. The operation layer includes both normal operation and fault operation states, with the optimization goal of minimizing the sum of normal operation costs and the fault costs associated with load shedding. Subsequently, a hybrid optimization algorithm combining an improved Aquila Optimizer-Second-Order Cone Programming (IAO-SOCP) is proposed to solve the coordinated optimization model. Finally, the proposed coordinated optimization method is validated using an enhanced IEEE 33-bus distribution network case study. The results demonstrate that the method effectively reduces network losses and minimizes load shedding costs during fault conditions, thereby ensuring a balance between the economic efficiency and reliability of the distribution network.

Keywords: active distribution network; distributed energy storage; dynamic reconstruction; coordinated optimization; improved aquila optimizer

Citation: Zhao, C.; Duan, Q.; Lu, J.; Wang, H.; Sha, G.; Jia, J.; Zhou, Q. Coordinated Optimization Method for Distributed Energy Storage and Dynamic Reconfiguration to Enhance the Economy and Reliability of Distribution Network. *Energies* **2024**, *17*, 6040. https://doi.org/10.3390/en17236040

Academic Editor: Santi A. Rizzo

Received: 4 November 2024
Revised: 25 November 2024
Accepted: 27 November 2024
Published: 1 December 2024

1. Introduction

As renewable energy sources, particularly wind and solar, are integrated into power systems, traditional distribution networks encounter unprecedented planning and operation challenges [1,2]. Distributed energy storage systems (DESS) have offered high controllability and economic benefits, significantly addressing flexibility challenges in distribution networks [3].

Several scholars have explored the application of distributed energy storage systems (DESS) in distribution networks. For instance, ref. [4] focuses on determining the optimal location, capacity, and power rating of batteries while minimizing costs subject to technical constraints. However, this study does not account for the impact of renewable energy capacity on DESS performance. In [5], a tri-level energy storage system planning approach is developed, which effectively enhances the robustness of forward-looking energy storage configurations against non-cooperative and uncertain renewable energy integration choices. Nonetheless, neither [4] nor [5] addresses the reliability of the distribution network. Ref. [6] introduces energy and frequency/expectation indexes to evaluate the reliability performance of the distribution system. It demonstrates that optimal energy storage allocation can enhance system reliability, but economic factors are not considered. Based on these, ref. [7] establishes a cost–benefit analysis-based optimal planning model for battery energy storage systems (BESS) in active distribution systems, taking into account the reliability improvement benefits of BESS during the planning phase.

In addition, the network structure of the distribution system remains static in the above studies. Dynamic reconfiguration is a core technology for actively managing distribution networks [8]. Ref. [9] proposes a load transfer capability analysis and network reconfiguration method applicable to large urban distribution networks with dynamic topology analysis, which is conducive to the balanced distribution of loads on multi-node distribution network contact lines but does not consider the occurrence of multiple faults in the distribution network. Ref. [10] proposes a resilience-oriented two-stage restoration considering coordinated maintenance and reconfiguration in integrated power distribution and heating systems, which demonstrates that dynamic reconfiguration can improve the efficiency of fault recovery through the synergy of the two phases of fault isolation and service restoration. Refs. [9,10] provide theoretical contributions to the study of dynamic reconfiguration of distribution networks, but neither of them considers the role played by energy storage in the fault reconfiguration process. Ref. [11] proposes a mixed-integer linear programming (MILP) joint planning model for ESS and distribution systems, focusing on minimizing the present value of annualized total investment while considering topology, construction, and operational constraints. It focuses on dynamic reconfiguration from an economic efficiency perspective but does not focus on the issue of distribution network reliability. In [12], a novel approach that considers the time-varying load restoration capability is proposed for the operational reliability assessment of distribution networks. The Risk of Customer Minutes Loss (RCML) and Risk of Energy Not Supplied (RENS) indices are firstly defined as the minimal load loss under the worst-case fault contingency in the upcoming time interval to evaluate the operational reliability. However, this literature has not investigated how to effectively coordinate and optimize the energy storage system with network reconstruction during multiple faults in the distribution network.

Based on these, scholars have studied the solution methods for DESS and distribution network reconfiguration. Ref. [13] proposes an improved particle swarm optimization algorithm, which has some global search capability but is sensitive to parameter settings, which can result in slower convergence if the settings are not reasonable. Ref. [14] proposes an improved bi-directional coevolutionary algorithm, which enhances the algorithm's convergence. Ref. [15] proposes a new novel radiality maintenance algorithm (RMA) that generates radial configurations by introducing a new concept of connected nodes and selection sets to improve the metaheuristic algorithm's standard deviation and computational efficiency. Aquila Optimizer (AO) [16] is an intelligent optimization algorithm proposed in recent years, which draws inspiration from the hunting behavior of eagles. Because it has multiple search strategies, it has excellent search capability as well as efficient optimization finding performance. Ref. [17] improves the Aquila Optimizer, significantly enhancing its initial convergence speed and achieving stronger global search capabilities.

Although the algorithms in the above literature have improved the performance to a certain extent, as heuristic algorithms, they generally suffer from the problems that the results are prone to fall into local optimal solutions and they require long computation time [18]. In contrast, commercial solvers can usually find the global optimal solution in a shorter time due to the highly optimized algorithms and efficient use of hardware resources, but they need to use decomposition algorithms or convex optimization techniques to transform the original non-convex planning problem into an easily solvable convex planning problem. For example, Ref. [19] uses Benders decomposition to divide the TEP problem into an investment master problem and many operation subproblems, which reduces the complexity of the problem and ensures global optimality, but the implementation of the algorithm is relatively complicated. Ref. [20] proposes a least squares approximation method to simplify the complex trigonometric functions in the dynamic power efficiency relationship of a bidirectional converter and convert the original non-convex relationship into a computationally efficient convex form. However, the poor fitting effect of the least squares method may lead to deviations in the model. Ref. [21] uses the GUROBI solver to solve a second-order conical model based on the Jordan framework for the reconfiguration of distribution networks containing energy storage systems. Ref. [22] uses Julia JuMP and GUROBI solver to validate the effectiveness of the joint planning model for energy storage systems and network reconfiguration. However, the computation time using only commercial solvers increases proportionally with the increase in distribution network node size, and the computational efficiency needs to be improved. Therefore, none of the existing solution methods can fully combine the advantages of heuristic algorithms and solvers, and there is an urgent need to improve the solution methods.

Furthermore, renewable energy sources have obvious uncertainties, and the multi-scenario generation technique is an effective method to analyze the power system uncertainty problem, which replaces the continuous probability density distribution function of the uncertainty of the output of distributed power sources, such as wind power and PV, with a large number of finite discrete deterministic samples and their corresponding probabilities [23], and then later reduces the similar scenarios to a finite number of typical scenarios [24]. Ref. [25] implements the generation of scenery-optimal scenes based on the Monte Carlo sampling method and removes redundant scenes using the synchronized backtracking elimination method. However, the method is computationally inefficient, and the computation time is long. Ref. [26] proposes a scenario-generation method based on the multivariate Copula function and greedy strategy to accurately characterize the correlation of power from multiple wind farms. Ref. [27] proposes a two-stage stochastic optimization approach to handle these uncertainties, and a scenario-based decomposition algorithm was developed to enhance the solution efficiency. However, the computational complexity is high, and the dependence on boundary conditions is strong. Latin Hypercubic Sampling (LHS), a stratified sampling method capable of generating sample points in a multidimensional parameter space, provides better coverage and efficiency than simple random sampling methods [28]. It covers a larger sampling space at the same computational scale and better robustness. Moreover, the Kantorovich distance with simultaneous backward elimination method to reduce the initial scenes can better preserve the probability distribution characteristics of the initial scenes and converge faster when the number of initial scenes is larger [29]. Therefore, the scene-generation method of LHS combined with Kantorovich distance reduction can improve the quality and efficiency of scene generation and reduction and has good application prospects.

In summary, this paper comprehensively considers both the economic performance of the active distribution network under normal conditions and the power supply reliability under fault conditions. A coordinated optimization method for distributed energy storage and dynamic reconstruction is proposed, which is aimed at improving the economic efficiency and reliability of the distribution network. Firstly, to capture the uncertainty associated with distributed resource output, a scenario-generation method utilizing Latin hypercube sampling and Kantorovich distance synchronous back-substitution reduction is presented. Next, a planning-operation layer coordinated optimization framework and a model that accounts for both normal and fault states of the distribution network are established. Finally, a hybrid optimization algorithm that combines the improved Aquila Optimizer with second-order cone programming is proposed to solve the coordinated optimization model. The effectiveness of this coordinated optimization method is validated using an enhanced IEEE 33-node distribution network example.

2. Materials and Methods

2.1. Multi-Scene Modelling Approach

As more sampling data obtained from scene generation will affect the computational speed and accuracy, and there are similarities between many scenes, scene reduction techniques can simplify similar scenes in the large number of initial scenes generated into a limited number of typical scenes, which can significantly reduce the computational amount while ensuring the accuracy of the model. The simultaneous back-generation elimination method using Kantorovich distance to reduce the initial scenes can better retain the probability distribution characteristics of the initial scenes and converge faster when the number of initial scenes is larger. The Kantorovich distance is defined as shown in Equation (1):

$$
\begin{aligned}
D_k\left(C_i, C_i^{\prime}\right) = \min \Bigg\{ & \sum_{s_v \in C_i, s_v^{\prime} \in C_i^{\prime}} d\left(s_v, s_v^{\prime}\right) \eta\left(s_v, s_v^{\prime}\right) \\
& \mid \ \eta\left(s_v, s_v^{\prime}\right) \geq 0, \forall s_v \in C_i, \forall s_v^{\prime} \in C_i^{\prime}; \\
& \sum_{s_v^{\prime} \in C_i^{\prime}} \eta\left(s_v, s_v^{\prime}\right) = p_{s_v}, \forall s_v \in C_i; \\
& \sum_{s_v \in C_i} \eta\left(s_v, s_v^{\prime}\right) = p_{s_v^{\prime}}, \forall s_v^{\prime} \in C_i^{\prime} \Bigg\}
\end{aligned} \tag{1}
$$

The steps of the Kantorovich-based scene reduction method are as follows:

(1) Scene initialization: set the original scene set C to represent the set of N retained scenes and the set of deleted scenes. Determine the initial probability p_{s_v} of retained scenes in set C as 1/N, and the initial probability $p_{s_v^{\prime}}$ of deleted scenes in set C as 1/ $N_i^{\prime}$;

(2) Determine the cut scenes $s_v^{\prime}$ and calculate the minimum value of the product of the distance between all scenes and their probabilities according to the Kantorovich distance, as shown in Equation (2). And categorize the scenes $s_v^{\prime}$ into the set $C_i^{\prime}$.

$$
D_k\left(C_i, C_i^{\prime}\right) = \min \left[\sum_{v=1}^{Av_i} p_{s_v} p_{s_v^{\prime}} d\left(s_v, s_v^{\prime}\right) \right] \tag{2}
$$

(3) Update the number of scenes by updating the initial number of scenes N_i to N_i−1 and deleting the number of scenes $N_i^{\prime} = N_i^{\prime}$ +1;

(4) Update the scene probability by selecting the scene nearest to s_v the scene through Equation (3) and updating the probability of the scene nearest $s_v^{\prime}$ to the removed scene $p_{s_v} = p_{s_v} + p_{s_v^{\prime}}$, so that the sum of probabilities of all scenes in the set of retained scenes C is 1. Then, update the probability of each scene in the set of deleted scenes to 1/ $N_i^{\prime}$;

$$
s_v = \arg\min \left[p_{s_v} p_{s_v^{\prime}} d\left(s_v, s_v^{\prime}\right) \right] \tag{3}
$$

(5) Go to step (2) and repeat the iteration until the number of scenes in the set of scenes C_i is cut down to the set number N.

Therefore, this paper adopts the Latin hypercube sampling method as well as the synchronous back-generation elimination method based on the Kantorovich distance to obtain the multi-scene modeling flow, as shown in Figure 1.

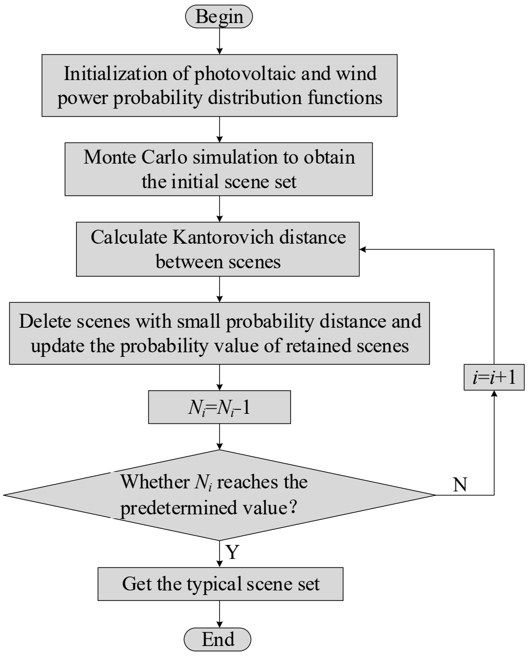

Figure 1. Flowchart of multi-scene modeling.

2.2. Coordination and Optimization Framework

To fully leverage the application potential of DESS and network reconfiguration, and to improve the economy of the distribution network in the normal state and the reliability of power supply in the fault state, a coordinated optimization framework based on distributed energy storage and dynamic reconfiguration is constructed, which includes two parts, namely, the site planning layer and the run operation layer, as shown in Figure 2.

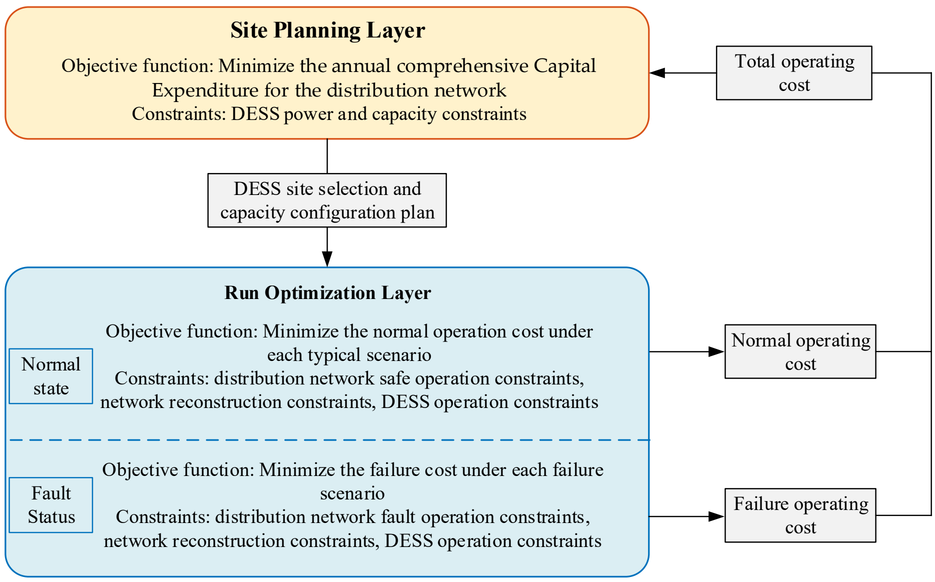

Figure 2. Coordinated optimization framework.

Among them, the site planning layer aims to minimize the annual comprehensive Capital Expenditures (CAPEX) for the distribution network to improve the distribution network economy, and the decision variables are the siting location and installation capacity of DESS. At the same time, the location and capacity of DESS are filtered under the satisfaction of DESS capacity constraints, power constraints, and security operation constraints such as voltage and current of the distribution network. The DESS power and capacity limitation constraints are shown in Formula (5), which means that the capacity and power of the DESS do not exceed the upper limit of the configuration, and the configured capacity and power are integer multiples of the unit capacity and power. The distribution network voltage and current constraints are shown in Formulas (8)–(15), which specifically include the network flow constraints of the distribution network and the constraints on voltage and current to keep the voltage within the specification value and not exceed the specified upper limit. The obtained DESS siting and capacity planning scheme is passed to the operation layer.

The run operation layer obtains typical scenarios based on Latin hypercubic sampling and the Kantorovich distance scenario-generation method and fully considers the two working conditions of normal state operation and fault state operation of the distribution network. Among them, the normal state operation layer aims to minimize the sum of DESS operation and maintenance costs, dynamic reconfiguration costs, and network loss costs under each typical scenario. It optimizes the DESS configuration plan in the planning layer with the lowest normal state operation cost as the goal. It obtains the optimal operating power and optimal dynamic reconfiguration plan of the DESS. The fault state operation layer considers the load transfer function of the DESS when a distribution network failure occurs and calculates the fault cost. The fault cost is calculated by considering the load-shifting effect of DESS when a fault occurs in the distribution network. The operation layer returns the sum of normal operation cost and fault cost to the planning layer, and feeds back the optimization results of the DESS operation power and branch currents. Finally, the two-layer models are iteratively optimized with each other to arrive at the optimal dynamic reconfiguration scheme and the DESS planning and operation scheme.

2.3. Coordination and Optimization Model

2.3.1. Site Planning Layer Model

(1) Objective function

The site planning layer model takes the minimization of the annual comprehensive CAPEX for the distribution network as the objective. The main consideration is the construction cost of DESS and the sum of the operating costs of the distribution network in normal and fault states, which is calculated by the formula:

$$\begin{cases} \min \quad F = Y_{\mathrm{IC}} + F_1 + F_2 \\ Y_{\mathrm{IC}} = \dfrac{\mu(1+\mu)^{y_{\mathrm{DES}}}}{(1+\mu)^{y_{\mathrm{DES}}}-1} \displaystyle\sum_{i\in\Phi_{\mathrm{D}}} [(c_{\mathrm{IN.D}}^{E} + c_{\mathrm{CON.D}})E_i^{\mathrm{DES}} \\ \qquad + c_{\mathrm{IN.D}}^{P} P_i^{\mathrm{DES}}] \end{cases} \tag{4}$$

where F is the annual comprehensive CAPEX for the distribution network; Y_{IC} is the construction cost of the DESS; F_1 is the operating cost of the distribution network in the normal state; F_2 is the operating cost of the distribution network in the fault state; y_{DES} is the economic service life of the DESS; μ is discount rate; Φ_{D} is the installation node set of the DESS; $c_{\mathrm{IN.D}}^{E}$ is equipment cost per unit capacity of the DESS; $c_{\mathrm{CON.D}}$ is construction cost per unit capacity of the DESS; $c_{\mathrm{IN.D}}^{P}$ is equipment purchase cost per unit power of the DESS.

(2) Constraints

The site planning layer model needs to satisfy the DESS capacity constraints and power constraints as:

$$\begin{cases} 0 \le E_i^{\mathrm{DES}} \le E_{i.\max}^{\mathrm{DES}} \text{ , } E_i^{\mathrm{DES}} = k_{i.\mathrm{E}}^{\mathrm{DES}} E_{\mathrm{N}}^{\mathrm{DES}} \\ 0 \le P_i^{\mathrm{DES}} \le P_{i.\max}^{\mathrm{DES}} \text{ , } P_i^{\mathrm{DES}} = k_{i.\mathrm{P}}^{\mathrm{DES}} P_{\mathrm{N}}^{\mathrm{DES}} \end{cases} \tag{5}$$

where E_i^{DES} and $E_{i.\max}^{\mathrm{DES}}$ is the capacity value and maximum capacity value of the DESS at node *i*, respectively; $E_{\mathrm{N}}^{\mathrm{DES}}$ is the unit capacity value of the DESS; P_i^{DES} and $P_{i.\max}^{\mathrm{DES}}$ is power value and maximum power value of the DESS at node *i*, respectively; $k_{i.\mathrm{E}}^{\mathrm{DES}}$ and $k_{i.\mathrm{P}}^{\mathrm{DES}}$ is number of units of capacity and power of the DESS at node *i*, both of which are non-negative integers.

2.3.2. Run Operation Layer Model

(1) Run operation layer

When the distribution network operates in the normal state, the economic optimality is considered, and this layer aims to minimize the sum of DESS operation and maintenance costs, dynamic reconfiguration costs, and network loss costs in each typical scenario. DESS operation and maintenance costs refer to the maintenance costs and operating costs incurred to ensure the normal operation of DESS and maintain its performance. The operating cost is mainly the cost of power loss during battery charging and discharging; while the maintenance cost is the cost of inspecting, maintaining, and repairing DESS. Dynamic reconstruction costs refer to the cost incurred by adjusting the network topology according to the distribution network. Specifically, it includes the cost of switch operation and power dispatching management required to achieve topology adjustment. Network loss costs refer to the economic cost caused by the loss of power during transmission in the distribution network. The objective function is as follows:

$$\begin{cases} \min \ F_1 = Y_{\mathrm{OM}} + Y_{\mathrm{D}} + Y_{\mathrm{L}} \\ Y_{\mathrm{OM}} = \lambda_{\mathrm{OM}} \sum_{m=1}^{M} \sum_{t=1}^{T} \sum_{i \in \Phi_{\mathrm{D}}} \left| P_{i,t,m}^{\mathrm{DES}} \right| \\ Y_{\mathrm{D}} = c_{\mathrm{sw}} \sum_{t=1}^{T} \left| \omega_{ij\ t} - \omega_{ij,t-1} \right| \\ Y_{\mathrm{L}} = D \sum_{m=1}^{M} \left[\left(\sum_{t=1}^{T} c_{\mathrm{B}} P_{ij,t,m}^{\mathrm{L}} \right) \bullet p_m \right] \end{cases} \tag{6}$$

where F_1 is the operating cost of the distribution network in the normal state; Y_{OM} is operation and maintenance cost of the DESS; Y_{D} is the dynamic restructuring cost of the distribution network; Y_{L} is the network loss cost; λ_{OM} is operation and maintenance cost coefficient of the DESS per unit power; $P_{i,t,m}^{\mathrm{DES}}$ is the active power of the DESS at node *i*; c_{sw} is cost of a single restructuring of the distribution network; $\omega_{ij\ t}$ is the switching state variable between branch *j* at time *t*; *D* is number of days for statistics; c_{B} is electricity price; $P_{ij,t,m}^{\mathrm{L}}$ is active power loss of branch *ij* at time *t*; p_m is the probability of scenario *m*.

(2) Fault state operation layer

$$F_2 = N_e \sum_{t=t_0}^{t_0+T_e} \sum_{j\in\Omega_N} c_l P_{j,t}^{L} \tag{7}$$

where N_e is the annual average fault frequency of the distribution network; c_l is load importance value coefficient; $P_{j,t}^{L}$ is the load outage amount at node *j* at time *t*; t_0 is fault start time; T_e is fault duration; Ω_N is set of nodes in the distribution network.

(3) Constraints

The constraints mainly contain network trend constraints and network security constraints, the specific calculation formula is shown below:

a. Network trend constraints

$$P_{i,t} = U_{i,t} \sum_{j=1}^{N} U_{j,t}(G_{ij}\cos\theta_{ij,t} + B_{ij}\sin\theta_{ij,t}) \tag{8}$$

$$Q_{i,t} = U_{i,t} \sum_{j=1}^{N} U_{j,t}(G_{ij}\sin\theta_{ij,t} - B_{ij}\cos\theta_{ij,t}) \tag{9}$$

$$P_{i,t} = P_{i,t}^{DG} - P_{i,t}^{DESS} - P_{i,t}^{\text{load}} \tag{10}$$

$$Q_{i,t} = Q_{i,t}^{DG} - Q_{i,t}^{DESS} - Q_{i,t}^{\text{load}} \tag{11}$$

$$I_{ij,t}^2 = (G_{ij}^2 + B_{ij}^2)(U_{i,t}^2 + U_{j,t}^2 - 2U_{i,t}U_{j,t}\cos\theta_{ij,t}) \tag{12}$$

where $P_{i,t}$ is active power injected at node *j* at time *t*; $Q_{i,t}$ is reactive power injected at node *j* at time *t*; $U_{i,t}$ is voltage magnitude at node *i* at time *t*; $U_{j,t}$ is voltage magnitude at node *j* at time *t*; G_{ij} is conductance in the admittance matrix at node *j*; B_{ij} is susceptance in the admittance matrix; $\theta_{ij,t}$ is voltage phase angle difference between nodes; $P_{i,t}^{DG}$ is active power output from distributed generation connected to node *i* at time *t*; $Q_{i,t}^{DG}$ is reactive power output from distributed generation connected to node *i* at time *t*; $P_{i,t}^{DESS}$ is active power output from DESS connected to node *i* at time *t*; $Q_{i,t}^{DESS}$ is active power output from DESS connected to node *i* at time *t*; $P_{i,t}^{\text{load}}$ is the active power of the load connected to node *i* at time *t*; $Q_{i,t}^{\text{load}}$ is the reactive power of the load connected to node *i* at time *t*; $I_{ij,t}$ is current in the branch *ij* at time *t*. The Formula (12) is derived from the relationship between node voltage and admittance, which can be found in reference [30].

b. Security constraints

$$U_{i,\min} \leqslant U_{i,t} \leqslant U_{i,\max} \tag{13}$$

$$s_{i,\min} \leqslant s_{i,t} \leqslant s_{i,\max} \tag{14}$$

$$I_{ij,t} \leqslant I_{ij,\max} \tag{15}$$

where $U_{i,\max}$ is the upper limit of the voltage at node *i*; $U_{i,\min}$ is the lower limit of the voltage at node *i*; $s_{i,\max}$ is the upper limit of the power at node *i*; $s_{i,\min}$ is the lower limit of the power; $I_{ij,\max}$ is the upper limit of the current in the branch *ij*.

c. Energy storage operational constraints

$$SOC_{i,t+1}^{\text{DES}} = SOC_{i,t}^{\text{DES}} + \frac{\eta_{\text{cha}} P_{i,t,\text{cha}}^{\text{DES}} K_{i,t,\text{cha}}^{\text{DES}}}{E_i^{\text{DES}}} + \frac{P_{i,t,\text{dis}}^{\text{DES}} K_{i,t,\text{dis}}^{\text{DES}}}{\eta_{\text{dis}} E_i^{\text{DES}}} \quad (16)$$

$$\begin{cases} 0 \le P_{i,t,\text{cha}}^{\text{DES}} \leqslant P_{i,\text{cha.max}}^{\text{DES}} \\ -P_{i,\text{dis.max}}^{\text{DES}} \le P_{i,t,\text{dis}}^{\text{DES}} \le 0 \\ K_{i,t,\text{cha}}^{\text{DES}} \cdot K_{i,t,\text{dis}}^{\text{DES}} = 0 \\ SOC_{i,1}^{\text{DES}} = SOC_{i,T+1}^{\text{DES}} \\ SOC_{\min}^{\text{DES}} \le SOC_{i,t}^{\text{DES}} \le SOC_{\max}^{\text{DES}} \end{cases} \quad (17)$$

where $SOC_{i,t}^{\text{DES}}$ is state of charge of the DESS at node *i* during time period *t*; η_{cha} and η_{dis} is charging and discharging efficiencies of the DESS, respectively; $P_{i,t,\text{cha}}^{\text{DES}}$ and $P_{i,t,\text{dis}}^{\text{DES}}$ is charging and discharging power of the DESS at node *i* during time period *t*, respectively; $K_{i,t,\text{cha}}^{\text{DES}}$ and $K_{i,t,\text{dis}}^{\text{DES}}$ is charging and discharging state indicators of the DESS at node *i* (0 for discharging and 1 for charging); $P_{i,\text{cha.max}}^{\text{DES}}$ and $P_{i,\text{dis.max}}^{\text{DES}}$ is maximum charging and discharging power of the DESS at node *i*, respectively; *T* is total number of time periods in a scheduling cycle; $SOC_{\max}^{\text{DES}}$ and $SOC_{\min}^{\text{DES}}$ is lower and upper limits of the state of charge.

d. Network dynamic reconfiguration constraints

The distribution network dynamic reconfiguration constraints include connectivity and radiality constraints and are free of islands and loops as shown in the following equation:

$$\begin{cases} \sum_{ij \in \psi_b} \omega_{ij} = n - 1 \\ \phi_{ij} + \phi_{ji} = \omega_{ij} \\ \sum_{j=1}^{J_N} \phi_{ij} = 1 \\ \phi_{1j} = 0 \end{cases} \quad (18)$$

where *n* is a number of branches in the distribution system; ϕ is a variable that indicates the subordination between nodes *i* and *j*; J_N is the total number of nodes in the system.

In addition, to ensure the economic operation of the distribution network and prolong the service life of the switch, the number of openings of the reconfiguration switch is limited, which can be expressed as follows:

$$\sum_{ij \in \psi_{\text{b}}} \left| \omega_{ij,t} - \omega_{ij,0} \right| \leqslant \chi_{\text{total}} \quad (19)$$

where χ_{total} is the maximum allowable number of operations (open/close actions) for all switches within the distribution network.

3. Solution Algorithms

Since the planning operation coordination optimization model established in this paper is a large-scale mixed-integer nonlinear planning model, it has the characteristics of variable nonlinearity. To improve the overall solution efficiency and convergence ability, the hybrid optimization algorithm of Improved Aquila Optimizer-Second-Order Cone Programming (IAO-SOCP) is used to solve the above model hierarchically. IAO is used for DESS pre-planning in the planning layer to obtain the optimal configuration location and capacity of DESS. In contrast, the operation layer is used for DESS pre-planning to obtain the optimal configuration location and capacity of DESS. The IAO is used for DESS pre-planning in the planning layer to obtain the optimal configuration location and capacity of DESS, while the SOCP method is used in the operation layer, which can solve the optimal operation scheme under different scenarios by transforming the complex non-convex model into a second-order cone model. The hybrid algorithm combining IAO and SOCP not only accelerates the convergence speed of the optimization algorithm but also improves the computational accuracy and stability of the overall solution.

3.1. Solution Algorithms of Aquila Optimizer

The idea of Aquila Optimizer (AO) originates from the predatory behavior of eagles in nature, which is divided into two phases: the exploration phase and the exploitation phase. Each phase has two strategies, and the probability of using different strategies is balanced by choosing random numbers. The predation strategy in the exploration stage is a high-altitude flight search and flying around the prey. The predation strategy in the exploitation stage is a low-altitude flight attack and ground proximity attack.

The exploration phase is executed when Equation (20) is satisfied, otherwise the exploitation phase is executed.

$$t \le \frac{2}{3}T \tag{20}$$

where t is the current iteration number and T is the maximum number of iterations.

(1) High-altitude flight searching

The Skyhawk in this strategy flies at high altitude to define the search space and find the best hunting area, expressed in a mathematical formula:

$$X(t+1) = X_{\text{best}}(t) \times \left(1 - \frac{t}{T}\right) + \left(X_{\text{M}}(t) - X_{\text{best}}(t) \times r_1\right) \tag{21}$$

$$X_M(t) = \frac{1}{N}\sum_{i=1}^{N} X_i(t) \tag{22}$$

where $X(t+1)$ is the position of the eagle in the next iteration; $X_{\text{best}}(t)$ is the position of the prey; $X_M(t)$ is the average position of the eagle population; r_1 is a random number ranging between 0 and 1; N is the size of the population.

(2) Flying around the prey

After determining the range of the prey, the Skyhawk will hover above in preparation for a landing attack, expressed in a mathematical formula:

$$X(t+1) = X_{\text{best}}(t) \times \text{LF}(D) + X_{\text{R}}(t) + (y - x) \times r_2 \tag{23}$$

where D is dimension; $X_{\mathrm{R}}(t)$ is a random position selected from the current population; r_2 is a random number ranging between 0 and 1; $\mathrm{LF(D)}$ is flight function, which can be calculated using the following formula:

$$\mathrm{LF}(D) = \mathrm{s} \times \frac{u \times \sigma}{|v|^{\frac{1}{\beta}}} \tag{24}$$

$$\sigma = \left(\frac{\Gamma(1+\beta) \times \sin\left(\frac{\pi\beta}{2}\right)}{\Gamma\left(\frac{1+\beta}{2}\right) \times \beta \times 2^{\left(\frac{\beta-1}{2}\right)}} \right)^{\frac{1}{\beta}} \tag{25}$$

where s is constant, equal to 0.01; u and v is random numbers ranging between 0 and 1; β is constant, equal to 1.5.

$$\begin{cases} x = l \times \sin(\theta) \\ y = l \times \cos(\theta) \\ l = C + 0.00565 \times D \\ \theta = -\omega \times D + \frac{3\pi}{2} \end{cases} \tag{26}$$

where C is the search space coefficient, ranging between 1 and 20; ω is constant, equal to 0.005.

(3) Low-flying attack

The Skyhawk descends vertically to make a preliminary attack on the prey, detecting the prey response, with the expression:

$$\begin{aligned} X(t+1) = (X_{\mathrm{best}}(t) - X_M(t)) \times \alpha - r_3 + \\ ((\mathrm{U_B}\text{-}\mathrm{L_B}) \times r_4 + \mathrm{L_B}) \times \delta \end{aligned} \tag{27}$$

where α and δ is values of the adaptive parameters, set to 0.1; $\mathrm{U_B}$ is the upper bound of the population; $\mathrm{L_B}$ is the lower bound of the population.

(4) Ground proximity attack

The Skyhawk comes to the ground and follows the movement of the prey to make a random catch; the expression is:

$$\begin{aligned} X(t+1) = \mathrm{QF}(t) \times X_{\mathrm{best}}(t) - G_1 \times X(t) \times r_5 - \\ G_2 \times \mathrm{LF}(D) + r_6 \times G_1 \end{aligned} \tag{28}$$

$$\mathrm{QF}(t) = t^{\frac{2 \times r_7 - 1}{(1-\mathrm{T})^2}} \tag{29}$$

$$G_1 = 2 \times r_8 - 1 \tag{30}$$

$$G_2 = 2 \times \left(1 - \frac{t}{\mathrm{T}}\right) \tag{31}$$

where $\mathrm{QF}(t)$ is the quality function of the balanced search strategy; G_1 is the motion parameter of the prey, a random number ranging between −1 and 1; G_2 is the flight slope of the eagle, linearly decreasing from 2 to 0; r_5, r_6, r_7, r_8 is the random numbers ranging between 0 and 1.

3.2. Improvement of Aquila Optimizer Algorithm

Although the AO algorithm has good optimization efficiency and solution accuracy, it may output local optimal solutions due to the randomness of the initial population, in this paper, we use the chaotic initialization strategy and the elite solution retention strategy to improve the Aquila Optimizer algorithm.

(1) Chaotic initialization strategy

Use the Tent map to construct the initial population, generating a population containing N_a chaotic individuals X_W. Use the following formula to calculate their reverse individuals O_W:

$$O_{\mathrm{w}} = r_3 \cdot (U_B + L_B) - X_{\mathrm{w}} \tag{32}$$

where r_3 is a random number ranging between 0 and 1.

When an individual goes out of bounds, update the reverse individual using the following formula:

$$O_{\mathrm{w}} = \mathrm{rand}(L_{\min}, L_{\max}) \tag{33}$$

Combine X_W and O_W to calculate the fitness, initializing the population with the individual that yields the optimal calculation result.

(2) Elite retention strategy

This strategy means that when the AO algorithm executes the next iteration, the elite solutions of the previous generation of populations are retained and merged, and the mixed populations are then arranged according to the fitness, which ensures that the individuals in the subgeneration of populations are all historically optimal solutions.

Firstly, the previous generation populations are arranged according to fitness; take the first half as W_1, the second half as W_2, and then perform the crossover operation on them according to the following equation:

$$\begin{cases} W_1' = R_1 \cdot W_1 + R_2 \cdot W_2 \\ W_2' = R_2 \cdot W_1 + R_1 \cdot W_2 \end{cases} \tag{34}$$

where W_1' and W_2' are the new populations generated after the crossover operation; R_1 and R_2 are random numbers ranging between 0 and 1.

Combine W_1' and W_2' to form a new population and select individuals based on fitness ranking. Finally, choose the top N_w individuals with the best fitness to proceed to the next iteration.

4. Results Analysis

4.1. Example Setup

In this paper, the simulation is carried out in the improved IEEE 33-node distribution network, which is a 10 kV medium voltage distribution network, as shown in Figure 3. A total of five PV units and four wind turbines are configured in the example, and the parameters are configured according to Table 1. The probabilistic distributions are set according to the light intensity and wind speed; the light intensity obeys the Beta distribution and the wind speed obeys the Weibull distribution. A total of three fault lines are set up, in which branch 15–16 has a fault period of 14:00–17:00, branch 7–8 has a fault period of 15:00–18:00, and branch 29–30 has a fault period of 16:00–19:00. The DESS configuration parameters are shown in Table 2. The time-of-day tariffs are shown in Table 3. The data on critical load demands is shown in Table 4. The load active power change curve is shown in Figure 4. The number of iterations of the improved Aquila Optimizer algorithm is set to 150.

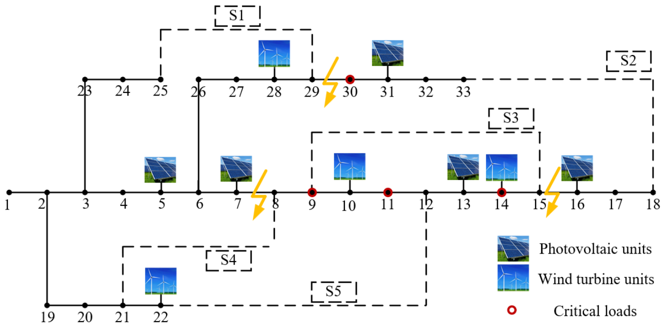

Figure 3. Improved IEEE 33-node distribution network.

Table 1. Wind turbine and photovoltaic configuration parameters

Connecting Unit	Connection Node Number	Capacity/kW
PV	5	100
	7	100
	13	200
	16	200
	31	200
WT	10	100
	14	100
	22	200
	28	400

Table 2. DESS configuration parameters

Parameters	Value
Discount rate	0.08
DESS state of charge upper limit	0.9
DESS state of charge lower limit	0.1
DESS charge/discharge efficiency	0.95
DESS economic service life/year	15
DESS equipment cost per unit capacity/(USD/kW h)	125
DESS investment cost per unit power/(USD/kW h)	70
DESS construction cost per unit capacity/(USD/kW h)	14
DESS operation and maintenance cost coefficient of per unit power/(USD/kW h)	5.6
Configured DESS maximum capacity/MW h	1
Configured DESS unit capacity/MW h	0.1
DESS configured maximum power/MW	1
DESS configured unit power/MW	0.1

Table 3. Time-of-use electricity prices.

Period Name	Time	Electricity Price/(USD/kW h)
Valley	0–7, 23–24	0.022
Flat	7–10, 12–16, 22–23	0.073
Peak	10–12, 16–17, 20–22	0.123

Super peak	17–20	0.149

Table 4. DATA on critical load demands.

Critical Load Node	Active Power (kW)	Reactive Power (kVar)
9	100	40
11	120	50
14	200	80
30	400	500

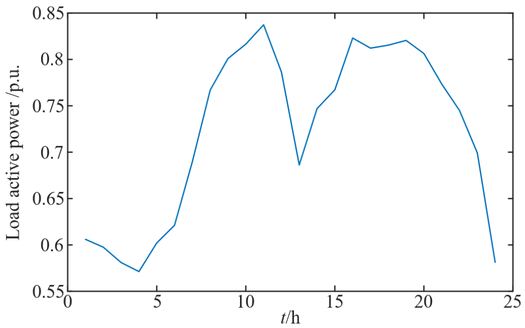

Figure 4. Load active power change curve.

4.2. Scene Generation Results

In this paper, we use Latin hypercubic sampling to generate 500 scenes of scenery outflow and then use the synchronous back-generation reduction method of Kantorovich distance for scene reduction of the above scenes to obtain five typical power scenario generation results, as shown in Figure 5.

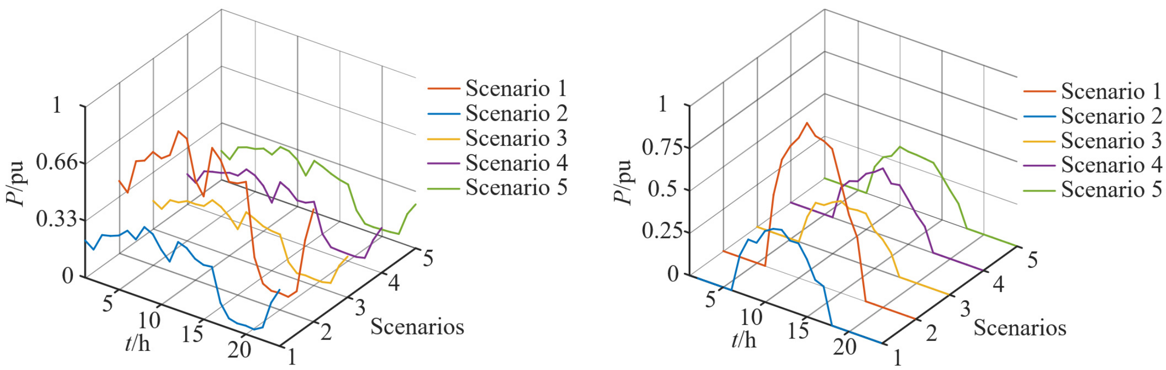

(**a**) (**b**)

Figure 5. Wind and solar power scenario generation results: (a) Wind power scenario generation results, (b) Solar power scenario generation results.

4.3. Analysis of Simulation Results

To verify the effectiveness of the coordinated planning model and the IAO-SOCP algorithm proposed in this paper, the example is generally solved based on MATLAB2018b software. Specifically, IAO is directly run in the MATLAB environment, and SOCP uses the YALMIP framework to call the GUROBI solver for the solution. The following three planning schemes are set up:

Scheme 1: No dynamic reconfiguration and no DESS configuration.

Scheme 2: No dynamic reconfiguration, but DESS is configured, but DESS only works in the normal state of the distribution network and exits during faults.

Scheme 3: Dynamic reconfiguration and DESS is configured, but DESS only works in the normal state of the distribution network and exits during faults.

Scheme 4: Dynamic reconfiguration and DESS are configured, and the coordination optimization method proposed in this paper is used to take into account both the normal state and the fault state of the distribution network.

4.3.1. Analysis of Results at the Planning Level

The planning results of the four schemes are shown in Figure 6 and Table 5, and the comparison of the total cost of different schemes is shown in Table 6. Combining the analysis of the figures and tables, it is evident that Scheme 1, which does not incorporate DESS and network reconfiguration, results in the highest total operating costs for the distribution network, ultimately affecting the overall cost. In Scheme 2, DESS is integrated at nodes 13, 22, and 28, all of which are locations with significant source-load power. This configuration effectively minimizes the peak-to-valley load difference, leading to the optimal economic performance of the distribution network under normal conditions, resulting in a total operating cost reduction of USD 26,470. Building on Scheme 2, Scheme 3 incorporates dynamic reconfiguration of the distribution network, altering the original network structure to improve power flow distribution in the spatial dimension. This change reduces both CAPEX and total operating costs of DESS. Compared to Scheme 2, the total cost in Scheme 3 decreases by USD 8450, a reduction of 1.83%. Scheme 4, in comparison to Scheme 3, features an increased total DESS capacity of 1.32 MWh and an additional power output of 0.98 MW. This enhancement is attributed to the coordinated optimization method proposed in this paper, which utilizes DESS in both normal and fault conditions to maximize its reliability during outages. Although Scheme 4 incurs an additional DESS CAPEX of USD 15,860, it still achieves a reduction in total operating costs. Consequently, the overall cost is reduced by USD 92,510 compared to Scheme 3, representing a 28.26% improvement, thereby enhancing both the economic efficiency and power supply reliability of the distribution network.

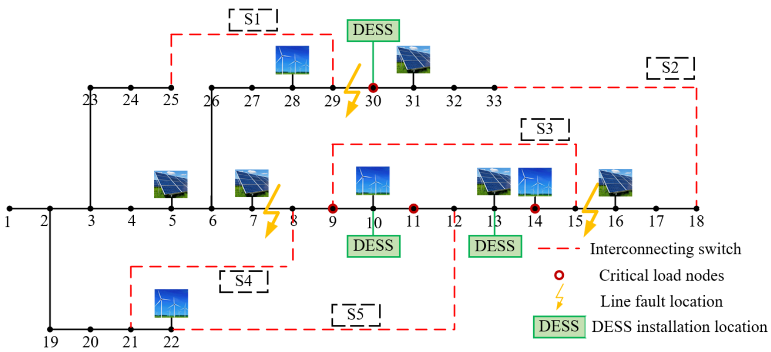

Figure 6. Planning configuration results under Scheme 4.

Table 5. Configuration results of different DESS schemes.

Scheme Number	Configuration Node	Power (MW)/Capacity (MW h)
2	13, 22, 28	0.1/0.4, 0.12/0.5, 0.2/0.8
3	10, 13, 28	0.06/0.3, 0.08/0.28, 0.14/0.5
4	10, 13, 30	0.4/0.8, 0.36/0.6, 0.5/1

Table 6. Configuration results of different DESS schemes.

Scheme Number	DESS CAPEX/10^4 USD	Total Operating Cost/10^4 USD	Total Cost/10^4 USD
1	0	46.086	46.086
2	1.802	43.439	45.241
3	1.199	31.540	32.739

4	2.785	20.703	23.488

4.3.2. Analysis of Operational Layer Results

Table 7 presents a comparative analysis of the operational costs for the three proposed schemes. Scheme 1, which does not incorporate any supply assurance resources, results in a complete power outage for critical loads during faults, especially in cases of multiple failures. Consequently, the fault costs incurred are significantly higher than the network loss costs during normal operation, accounting for 80.91% of the total operating costs. In contrast, Schemes 2 to 4 integrate DESS, demonstrating a significant impact on reducing network loss costs. Scheme 2 focuses solely on the operation of DESS during normal conditions, transferring source-load power over time, which effectively lowers the overall network loss costs; however, the fault costs due to outages remain unchanged. Building upon this, Schemes 3 and 4 implement dynamic reconfiguration of the distribution network. This spatial flexibility in power flow further reduces network loss costs, indicating that the combination of DESS with network dynamic reconfiguration offers superior economic benefits.

Table 7. Comparison of operating costs of different schemes.

Scheme Number	DESS Operation and Maintenance Cost/10^4 USD	Network Loss Cost/10^4 USD	Dynamic Reconfiguration Cost/10^4 USD	Failure Cost/10^4 USD	Total Operating Cost/10^4 USD
1	0	8.798	0	37.288	46.086
2	0.896	5.255	0	37.288	43.439
3	0.648	3.738	1.673	25.481	31.540
4	1.436	3.504	1.561	21.202	27.703

Through the comparative analysis of Scheme 2 and Scheme 3, the impact of dynamic reconfiguration of the distribution network on DESS planning can be seen more clearly. There is little change in the location configuration of DESS between the two schemes, but in Scheme 3, the capacity and power of DESS configured everywhere are significantly reduced. This change is mainly due to the introduction of dynamic reconfiguration, which re-adjusts the grid structure of the distribution network, thereby optimizing the spatial distribution of power flow. Specifically, dynamic reconfiguration effectively alleviates local load pressure and enhances the system's load-balancing capability by reconfiguring the power flow direction, thereby reducing the demand for DESS capacity. This not only reduces the initial DESS CAPEX but also effectively controls the total operating cost of the distribution network. Under the optimization of Scheme 3, the distribution of power flow in the spatial dimension of the distribution network is more reasonable, and resource utilization is more efficient, thus significantly improving the overall economy and operating efficiency.

Comparing Schemes 3 and 4, we analyze the impact of DESS power support and the alternative supply paths provided by network dynamic reconfiguration on the planning outcomes during fault conditions. Scheme 4 shows a reduction in fault costs of USD 42,790, a decrease of 32.55% compared to Scheme 3. This reduction can be attributed to the fact that the amount of load that can be supported during a fault is limited by the capacity of the DESS; a larger DESS capacity is more advantageous in minimizing the outage load of the faulted feeder, thereby reducing fault costs. Thus, it can be concluded that while the planning scheme that considers fault costs increases the investment and maintenance costs for DESS, it effectively leverages the benefits of DESS in reducing load outage losses and enhancing the reliability of the distribution system.

Figure 7 illustrates the operational power and state of charge (SOC) variations of the DESS configured at different locations in Scheme 4. As shown in the figure, all DESS units charge during low electricity price periods from 0 to 7 h and 23 to 24 h, and discharge during peak and high-peak hours from 16 to 20 h. This indicates that the DESS can temporally shift source-load power, thereby reducing the peak-to-valley load difference and enhancing the overall economic efficiency of the distribution network. Additionally, the distribution network experiences multiple line faults between 14 and 18 h, during which all three DESS units discharge to mitigate the losses associated with load outages. This action not only increases the reliability of the distribution system but also meets the dual demands of economic efficiency and reliability for the distribution network.

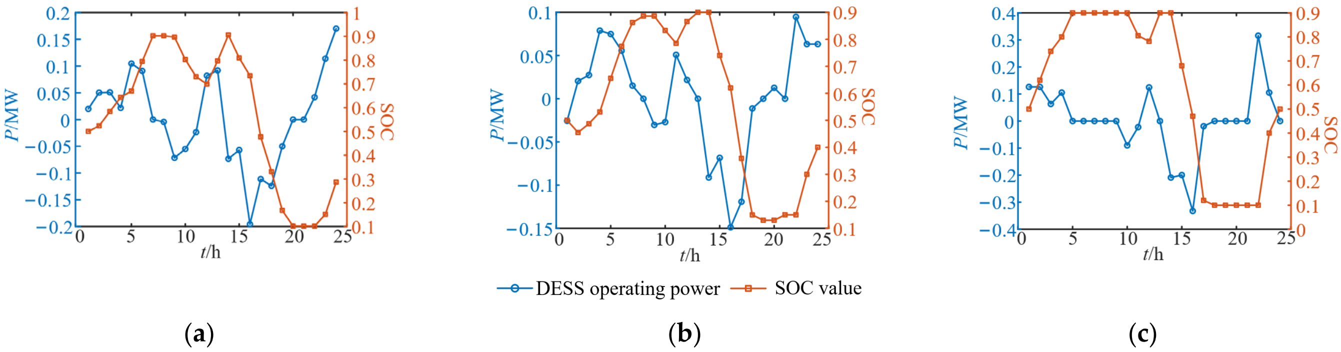

Figure 7. Planning configuration results under Scheme 4: (**a**) at node 10, (**b**) at node 13, and (**c**) at node 30.

The dynamic reconstruction line numbers and change periods for Scheme 3 and Scheme 4 are shown in Figure 8. Compared to Scheme 1, where the grid structure cannot be altered and is not flexible enough, leading to higher network losses, Schemes 3 and 4 incorporate dynamic reconstruction, providing the distribution network with greater flexibility. This allows for the adjustment of power supply paths based on the real-time operational status and load demands of the distribution network. During normal conditions, it seeks the most economically optimal path, while in the event of a fault, it finds the path with the highest reliability. Due to the limitation on the maximum number of reconstructions, adjustments are made during peak load variation periods in the early morning and evening. Scheme 4 requires fewer reconstructions than Scheme 3, as it has a larger capacity, enabling more flexible load and flow transfers without the need to frequently change the grid structure.

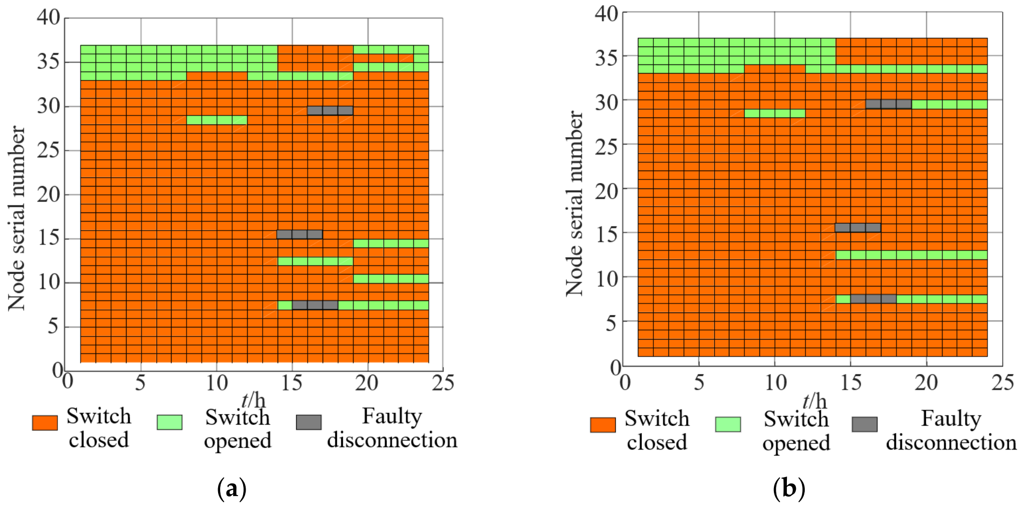

Figure 8. Dynamic restructuring results: (**a**) Scheme 3, (**b**) Scheme 4.

Analyze the distribution network reconstruction and load recovery in Table 8. Since the fault points set in this paper are located at three different locations and last for different periods, the load disconnected after the faults at 14~15 h and 17~18 h can be restored through network reconstruction, and the power supply is achieved by closing the switches at S2, S3, and S4. At 16 h, due to the simultaneous occurrence of three faults and the fault location restrictions at lines 29–30 and 15–16, the load cannot be restored through reconstruction, resulting in a large power loss cost. During the fault, the switches S2, S3, S4 all became closed. This is because the power supply of the critical loads is guaranteed first. The switch at S2 guarantees the load at node 30, and the switches at S3 and S4 guarantee the power supply of the critical loads at nodes 9, 11, and 14. At the same time, the switches at 12–13 are disconnected to ensure that no ring network is generated. From the above analysis, it can be seen that distribution network reconstruction can guarantee load power supply to the greatest extent.

Table 8. Fault reconstruction and load recovery under scheme 4.

Time/h	Fault line number	Restructure line number Switch off	Restructure line number Switch on	Node number of restore load
14	15–16	S2, S3, S4	7–8, 12–13	16, 17, 18
15	7–8, 15–16	S2, S3, S4	12–13	8~15
16	7–8, 15–16, 29–30	S2, S3, S4	12–13	-
17	7–8, 29–30	S2, S3, S4	12–13	30~33
18	29–30	S2, S3, S4	7–8,12–13	30~33

4.3.3. Comparison of Different Algorithm Simulations

To verify the superiority of the improved Aquila Optimizer algorithm proposed in this paper, comparisons were made with the Genetic algorithm and the traditional Aquila Optimizer algorithm. The results of different solving algorithms are shown in Table 9, and the iterative curves for various algorithms are depicted in Figure 9. Analyzing both the figure and the table, the average number of iterations of the proposed improved algorithm is reduced by 3.9% and 20.1% compared to the Aquila Optimizer and Genetic algorithm, respectively, and the convergence times decreased by 39.5% and 62.4%. This confirms that the chaotic initialization and elite solution retention strategy enhance the global search capability of the Aquila Optimizer algorithm while accelerating its convergence speed.

Table 9. Comparison of results from different solving algorithms.

Algorithm	DESS CAPEX/Ten Thousand USD	Average Iteration Count/Times	Average Convergence Time/Seconds
Genetic Algorithm	3.034	46	642.85
Aquila Optimizer	2.906	35	359.12
Improved Aquila Optimizer	2.785	27	243.47

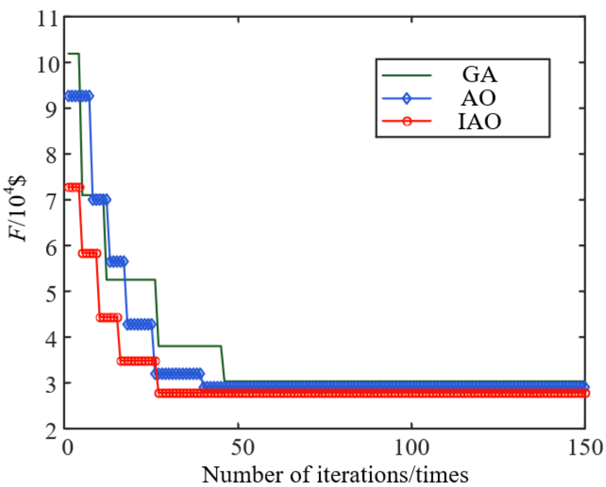

Figure 9. Iteration curves of different algorithms.

5. Conclusions

To enhance the economic efficiency of distribution networks under normal conditions and the reliability of power supply during fault conditions, a coordinated optimization method utilizing DESS and dynamic reconfiguration has been proposed. Through comparative analysis of case studies, the following conclusions can be drawn:

(1) The proposed coordinated optimization method aims to minimize the comprehensive CAPEX for the distribution network at the planning layer to improve the economic efficiency of the distribution network. At the operational layer, the objective is to minimize the sum of normal operating costs and the costs associated with load outages during faults. The simulation results show that the coordinated optimization of DESS and dynamic reconstruction comprehensively improves the economy of distribution station operation, reduces the fault cost, and ensures power supply reliability.

(2) The proposed optimization model incorporates both the normal operation layer and the fault operation layer, enabling a combination of normal operational costs and costs incurred during fault conditions. By utilizing DESS for discharge during faults and dynamically reconfiguring the network, power support can be provided to critical loads from both temporal and spatial dimensions. Compared to schemes that do not consider fault costs, the proposed method results in a 32.55% reduction in fault costs and a 32.14% reduction in total operating costs, thereby ensuring reliable power supply to critical loads.

(3) The proposed improved Aquila Optimizer-Second-Order Cone Programming (IAO-SOCP) combines chaotic initialization with the elite solution retention strategy, which can enhance the randomness of the algorithm and jump out of the local optimum more quickly. Compared with the Aquila Optimizer and Genetic algorithm, the number of iterations is reduced by 8 and 19 times, respectively, and the convergence time is reduced by 32.2% and 62.1%, respectively, which verifies that the improved algorithm can improve the overall search efficiency and convergence performance.

This paper has studied the method of distributed energy storage system and dynamic reconstruction of the distribution network, which shows that the coordinated optimization of the two can improve the economy and reliability of the distribution network. The distributed resources in this paper focus on battery energy storage. In the future, we will study how to comprehensively optimize various types of distributed resources (such as fuel cells and diesel engines) to be closer to the application scenarios of actual distribution networks.

Author Contributions: Conceptualization, C.Z. and Q.D.; methodology, C.Z. and J.L.; software, H.W. and J.J.; validation, H.W., G.S. and J.J.; formal analysis, Q.Z.; investigation, Q.D.; resources, J.L.; data curation, G.S.; writing—original draft preparation, J.J.; writing—review and editing, C.Z.; visualization, Q.D.; supervision, H.W.; project administration, J.J.; funding acquisition, Q.Z. All authors have read and agreed to the published version of the manuscript.

Funding: This research was funded by the Science and Technology Project of State Grid (5108-202218280A-2-376-XG).

Data Availability Statement: Data are contained within the article.

Acknowledgments: The authors gratefully thank the financial support of the Science and Technology Project of State Grid (5108-202218280A-2-376-XG).

Conflicts of Interest: Qi Zhou was employed by the Electric Power Science Research Institute of State Grid Jiangsu Electric Power Company. The remaining authors declare that the research was conducted in the absence of any commercial or financial relationships that could be construed as a potential conflict of interest.

Nomenclature

D_k	Kantorovich distance
C_i, $C_i^{'}$	Collection of original and deleted scenes
s_v, $s_v^{'}$	Scenarios in sets C_i and $C_i^{'}$
p_{s_v}, $p_{s_v^{'}}$	Probability of scenarios s_v and $s_v^{'}$
F	annual comprehensive CAPEX for the distribution network
Y_{IC}	construction cost of the DESS
F_1	operating cost of the distribution network in the normal state
F_2	operating cost of the distribution network in the fault state
y_{DES}	economic service life of the DESS
μ	discount rate
Φ_{D}	installation node set of the DESS
$c_{\mathrm{IN.D}}^{E}$	equipment cost per unit capacity of the DESS
$c_{\mathrm{CON.D}}$	construction cost per unit capacity of the DESS
$c_{\mathrm{IN.D}}^{P}$	equipment purchase cost per unit power of the DESS
E_i^{DES}	capacity value of the DESS
$E_{i.\max}^{\mathrm{DES}}$	maximum capacity value of the DESS
$E_{\mathrm{N}}^{\mathrm{DES}}$	unit capacity value of the DESS
P_i^{DES}	power value of the DESS
$P_{i.\max}^{\mathrm{DES}}$	the maximum power value of the DESS
$k_{i.\mathrm{E}}^{\mathrm{DES}}$, $k_{i.\mathrm{P}}^{\mathrm{DES}}$	number of DESS per unit capacity and power
Y_{OM}	operation and maintenance cost of the DESS
Y_{D}	dynamic restructuring cost of the distribution network
Y_{L}	network loss cost
λ_{OM}	operation and maintenance cost coefficient of the DESS per unit power
$P_{i,t,m}^{\mathrm{DES}}$	active power of the DESS
c_{sw}	cost of a single restructuring of the distribution network
$\omega_{ij\ t}$	switching state variable
D	number of days for statistics
c_{B}	electricity price
$P_{ij,t,m}^{\mathrm{L}}$	active power loss of branch *ij*
p_m	probability of scenario *m*
N_{e}	annual average fault frequency of the distribution network
c_l	load importance value coefficient
$P_{j,t}^{\mathrm{L}}$	load outage amount at node *j* at time *t*
t_0	fault start time
T_{e}	fault duration
Ω_{N}	set of nodes in the distribution network
$P_{i,t}$, $Q_{i,t}$	active power and reactive power injected from node *i*
$U_{i,t}$, $U_{j,t}$	voltage magnitude at node *i* and node *j*
G_{ij}, B_{ij}	conductance and susceptance in the admittance matrix
$\theta_{ij,t}$	voltage phase angle difference between nodes

$P_{i,t}^{DG}$ $Q_{i,t}^{DG}$	active power and reactive power output from distributed generation
$P_{i,t}^{DESS}$, $Q_{i,t}^{DESS}$	active power and reactive power output from DESS
$P_{i,t}^{\text{load}}$, $Q_{i,t}^{\text{load}}$	active power and reactive power of the load
$I_{ij,t}$	current in the branch
$U_{i,\max}$, $U_{i,\min}$	the upper limit and lower limit of the voltage
$s_{i,\max}$, $s_{i,\min}$	the upper limit and lower limit of the power
$I_{ij,\max}$	the upper limit of the current in the branch *ij*
$SOC_{i,t}^{\text{DES}}$	state of charge of the DESS
η_{cha}, η_{dis}	charging and discharging efficiencies of the DESS
$P_{i,t,\text{cha}}^{\text{DES}}$, $P_{i,t,\text{dis}}^{\text{DES}}$	charging and discharging power of the DESS
$K_{i,t,\text{cha}}^{\text{DES}}$, $K_{i,t,\text{dis}}^{\text{DES}}$	charging and discharging state indicators of the DESS
$P_{i,\text{cha.max}}^{\text{DES}}$, $P_{i,\text{dis.max}}^{\text{DES}}$	maximum charging and discharging power of the DESS
$SOC_{\max}^{\text{DES}}$, $SOC_{\min}^{\text{DES}}$	lower and upper limits of the state of charge
n	number of branches in the distribution system
ϕ	variable that indicates the subordination between nodes *i* and *j*
J_N	total number of nodes in the system
χ_{total}	maximum allowable number of operations for all switches within the distribution network

References

1. Zhang, N.; Xu, Z.; Zhong, C.; Jia, L.; Yao, K.; Li, J.; Sun, C.; Yuan, R.; Zheng, B.; Shao, L.; et al. Collaborative optimization scheduling of active distribution networks in mountainous areas based on improved particle swarm optimization algorithm. In Proceedings of the 2024 3rd International Conference on Energy, Power and Electrical Technology (ICEPET), Chengdu, China, 17–19 May 2024; pp. 622–627.
2. Torres, B.S.; Borges da Silva, L.E.; Salomon, C.P.; de Moraes, C.H.V. Integrating Smart Grid Devices into the Traditional Protection of Distribution Networks. *Energies* **2022**, *15*, 2518.
3. Fang, J.; Pei, Z.; Chen, T.; Peng, Z.; Kong, S.; Chen, J.; Huang, S. Economic benefit evaluation model of distributed energy storage system considering custom power services. *Front. Energy Res.* **2023**, *10*, 1029479.
4. Sedghi, M.; Ahmadian, A.; Aliakbar-Golkar, M. Optimal storage planning in active distribution network considering uncertainty of wind power distributed generation. *IEEE Trans. Power Syst.* **2016**, *31*, 304–316.
5. Cao, X.; Cao, T.; Gao, F.; Guan, X. Risk-Averse Storage Planning for Improving RES Hosting Capacity under Uncertain Siting Choices. *IEEE Trans. Sustain. Energy*. **2021**, *12*, 1984–1995.
6. Tur, M.R. Reliability assessment of distribution power system when considering energy storage configuration technique. *IEEE Access* **2020**, *8*, 77962–77971.
7. Liu, W.; Niu, S.; Xu, H. Optimal planning of battery energy storage considering reliability benefit and operation strategy in active distribution system. *J. Mod. Power Syst. Clean Energy* **2017**, *5*, 177–186.
8. Santos, S.; Gough, M.; Fitiwi, D.Z.; Pogeira, J.; Shafie-Khah, M.; Catalao, J. Dynamic Distribution System Reconfiguration Considering Distributed Renewable Energy Sources and Energy Storage Systems. *IEEE Syst. J.* **2022**, *16*, 3723–3733.
9. Li, Z.; Shi, D.; Huo, J.; Chen, K.; Shao, M.; Sun, W. Research on Load-Transfer Capacity Analysis and Network Reconstruction Method for Large City Distribution Networks. In Proceedings of the 2023 IEEE 7th Conference on Energy Internet and Energy System Integration (EI2), Hangzhou, China, 15–18 December 2023; pp. 417–422.
10. Wang, K.; Xue, Y.; Shahidehpour, M.; Chang, X.; Li, Z.; Zhou, Y.; Sun, H. Resilience-Oriented Two-Stage Restoration Considering Coordinated Maintenance and Reconfiguration in Integrated Power Distribution and Heating Systems. *IEEE Trans. Sustain. Energy*. Early Access, **2024**, 1–13. DOI: 10.1109/TSTE.2024.3434995.
11. Bosisio, A.; Berizzi, A.; Lupis, D.; Morotti, A.; Iannarelli, G.; Greco, B. A Tabu-search-based Algorithm for Distribution Network Restoration to Improve Reliability and Resiliency. *J. Mod. Power Syst. Clean Energy* **2023**, *11*, 302–311.
12. Yin, H.; Wang, Z.; Liu, Y.; Qudaih, Y.; Tang, D.; Liu, J.; Liu, T. Operational Reliability Assessment of Distribution Network With Energy Storage Systems. *IEEE Syst. J.* **2023**, *17*, 629–639.

13. Li, T.; Ge, J.; Zhu, R. Distribution Network Reconfiguration Based on Improved Particle Swarm Optimization Algorithm. In Proceedings of the 2024 3rd International Conference on Energy, Power and Electrical Technology (ICEPET), Chengdu, China, 17–19 May 2024; pp. 746–749.
14. Ali, A.; Liu, Z.; Ali, A.; Abbas, G.; Touti, E.; Nureldeen, W. Dynamic Multi-Objective Optimization of Grid-Connected Distributed Resources Along with Battery Energy Storage Management via Improved Bidirectional Coevolutionary Algorithm. *IEEE Access* **2024**, *12*, 58972–58992.
15. Iqbal, M.A.; Zafar, R. A Novel Radiality Maintenance Algorithm for the Metaheuristic Based Co-Optimization of Network Reconfiguration with Battery Storage. *IEEE Access* **2023**, *11*, 25689–25701.
16. Meng, Z.; Jin, X.; Liu, J.; Cai, X.; Zhu, J.; Pan, T. Electric Vehicle Load Control Strategy Based on Improved Aquila Optimizer Algorithm. In Proceedings of the 2023 6th Asia Conference on Energy and Electrical Engineering (ACEEE 2023), Chengdu, China, 21–23 July 2023; pp. 372–376.
17. Verma, M.; Sreejeth, M.; Singh, M.; Babu, T.S.; Alhelou, H.H. Chaotic Mapping Based Advanced Aquila Optimizer With Single Stage Evolutionary Algorithm. *IEEE Access* **2022**, *10*, 89153–89169.
18. Li, P.; Ji, H.; Wang, C.; Zhao, J.; Song, G.; Ding, F.; Wu, J. Coordinated Control Method of Voltage and Reactive Power for Active Distribution Networks Based on Soft Open Point. *IEEE Trans. Sustain. Energy* **2017**, *8*, 1430–1442.
19. Zhuo, Z.; Du, E.; Zhang, N.; Kang, C.; Xia, Q.; Wang, Z. Incorporating Massive Scenarios in Transmission Expansion Planning with High Renewable Energy Penetration. *IEEE Trans. Power Syst.* **2020**, *35*, 1061–1074.
20. Liang, Z.; Chung, C.Y.; Zhang, W.; Wang, Q.; Lin, W.; Wang, C. Enabling High-Efficiency Economic Dispatch of Hybrid AC/DC Networked Microgrids: Steady-State Convex Bi-Directional Converter Models. *IEEE Trans. Smart Grid.* Early Access, **2024**, 1-17. DOI: 10.1109/TSG.2024.3454050.
21. Cui, Z.; Bai, X.; Li, P.; Cao, Y.; Diao, Z. Reconfiguration of distribution network based on Jordan frames with energy storage system, In Proceedings of the 2017 IEEE Conference on Energy Internet and Energy System Integration (EI2), Beijing, China, 26–28 November 2017; pp. 1–6.
22. Dong, S.; Zhou, T.; Li, W.; Ye, L.; Zhao, N.; He, G.; Geng, G. Joint Planning of Energy Storage and Distribution System Considering Network Reconfiguration. In Proceedings of the 2023 IEEE 7th Conference on Energy Internet and Energy System Integration (EI2), Hangzhou, China, 15–18 December 2023; pp. 148–152.
23. Mosbah, M.; Arif, S.; Mohammedi, R.D.; Hellal, A. Optimum dynamic distribution network reconfiguration using minimum spanning tree algorithm. In Proceedings of the 2017 5th International Conference on Electrical Engineering—Boumerdes (ICEE-B), Boumerdes, Algeria, 29–31 October 2017; pp. 1–6.
24. Kini, K.R.; Bapat, M.; Madakyaru, M. Kantorovich Distance Based Fault Detection Scheme for Non-Linear Processes. *IEEE Access* **2022**, *10*, 1051–1067.
25. Xu, C.; Xu, Z.; Shi, L.; Xu, J.; Guan, X.; & Xiao, F. Typical Scenario Generation Method for Integrated Energy Systems Considering Spatio-Temporal Properties. In Proceedings of the 2023 IEEE 7th Conference on Energy Internet and Energy System Integration (EI2), Hangzhou, China, 15–18 December 2023; pp. 855–860.
26. Cheng, D.; Xing, F.; Su, R.; Qi, H.; Ma, L.; Ma, H.; Wang, T.; Zhou, N.; Li, C. Multiple Wind Farms Power Generation Scenario Generation and Reduction Based on Multivariate Copula Function and Greedy Strategy. In Proceedings of the 2023 7th International Conference on Power and Energy Engineering (ICPEE), Chengdu, China, 22–24 December 2023, 337–342.
27. Li, W.; Zou, Y.; Yang, H.; Fu, X.; Sheng, Xiang, Li, Z. Two-stage Stochastic Energy Scheduling for Multi Energy Rural Microgrids With Irrigation Systems and Biomass Fermentation. *IEEE Trans. Smart Grid.* Early Access, **2024**, 1-12. DOI: 10.1109/TSG.2024.3483444.
28. He, Z.; Zhang, Y.; Zheng, G.; Zheng, F.; Jin, W. Impact Analysis of High Proportion of PV Access on Distribution Network. In Proceedings of the 2022 12th International Conference on Power and Energy Systems (ICPES 2022), Guangzhou, China, 23–25 December 2022; pp. 810–815.
29. Ai, X. Design and Optimization of Power System Day-Ahead Scheduling Based on Kantorovich Algorithm. In Proceedings of the 2024 6th International Conference on Energy Systems and Electrical Power (ICESEP 2024), Guangzhou, China, 21–23 June 2024; pp. 509–512.
30. Dong, X.; Wu, Z.; Song, G.; Ji, H.; Li, P.; Wang, C. A hybrid optimization algorithm for distribution network coordinated operation with SNOP based on simulated annealing and conic programming. In Proceedings of the 2016 IEEE Power and Energy Society General Meeting (PESGM), Boston, MA, USA, 17–21 July 2016; pp. 1–5.